Neurological Sciences (2019) 40:993–1000
https://doi.org/10.1007/s10072-019-03751-4

ORIGINAL ARTICLE

Source localization of epileptiform discharges in childhood absence epilepsy using a distributed source model: a standardized, low-resolution, brain electromagnetic tomography (sLORETA) study

Ye-Hwa Jun[1] · Tae-Hoon Eom[1] · Young-Hoon Kim[1] · Seung-Yun Chung[1] · In-Goo Lee[1] · Jung-Min Kim[2]

Received: 22 September 2018 / Accepted: 4 February 2019 / Published online: 12 February 2019

Abstract

Localizing the source of epileptiform discharges in generalized epilepsy has been controversial for the past few decades. Recent neuroimaging studies have shown that epileptiform discharges in generalized epilepsy can be localized to a particular region. Childhood absence epilepsy (CAE) is the most common generalized epilepsy in childhood and is considered the prototype of idiopathic generalized epilepsy (IGE). To better understand electrophysiological changes and their development in CAE, we investigated the origin of epileptiform discharges. We performed distributed source localization with standardized, low-resolution, brain electromagnetic tomography (sLORETA). In 16 children with CAE, sLORETA images corresponding to the midpoint of the ascending phase and the negative peak of the spike were obtained from a total of 242 EEG epochs (121 epochs at each timepoint). Maximal current source density (CSD) was mostly located in the frontal lobe (69.4%). At the gyral level, maximal CSD was most commonly in the superior frontal gyrus (39.3%) followed by the middle frontal gyrus (14.0%) and medial frontal gyrus (8.7%). At the hemisphere level, maximal CSD was dominant in the right cerebral hemisphere (63.6%). These results were consistent at the midpoint of the ascending phase and the negative peak of the spike. Our results demonstrated that the major source of epileptiform discharges in CAE was the frontal lobe. These results suggest that the frontal lobe is involved in generating CAE. This finding is consistent with recent studies that have suggested selective cortical involvement, especially in the frontal regions, in IGE.

Keywords Childhood absence epilepsy (CAE) · Electroencephalography (EEG) · Source localization · Distributed source model · Standardized, low-resolution, brain electromagnetic tomography (sLORETA)

Introduction

Epilepsy is broadly classified into generalized and focal epilepsy. Generalized epilepsy involves diffuse and bilateral cerebral regions, whereas focal epilepsy is associated with focal or multifocal brain regions involving one hemisphere. Idiopathic generalized epilepsy (IGE) is a subgroup of generalized epilepsy with no evidence of structural brain lesions [1].

Childhood absence epilepsy (CAE) is the most common generalized epilepsy syndrome in childhood and is considered the prototype of IGE. CAE consists of typical absence seizures, and EEG demonstrates characteristic "generalized 3-Hz spike and wave complexes" [2]. The thalamic stimulation model was the first experimental model for the spike-wave pattern [3, 4]. This model posits that abnormal oscillatory rhythms in a thalamocortical circuit generate and sustain generalized spike-wave discharges, and it explains the generalized nature of the pathophysiology of CAE [5–7]. However, spike-wave patterns in CAE have been reported as not diffuse but predominant in the frontal cortex [8–10]. Moreover, epileptiform discharge in CAE may appear fragmentary, especially during sleep, and focal spikes may occur over the centrotemporal and occipital regions [11].

Electronic supplementary material The online version of this article (https://doi.org/10.1007/s10072-019-03751-4) contains supplementary material, which is available to authorized users.

✉ Tae-Hoon Eom
good1976@hanmail.net

[1] Department of Pediatrics, College of Medicine, The Catholic University of Korea, Seoul, Republic of Korea

[2] Department of Internal Medicine, Sanggye Paik Hospital, College of Medicine, Inje University, Seoul, Republic of Korea

Currently, the thalamocortical theory of CAE is widely accepted, although the relative contributions of the cortex and thalamus and the underlying mechanisms remain matters of debate. Various authors have suggested various origins or source locations of epileptic activity, based on animal experiments and human studies, from various cortical or subcortical structures [5, 12–14].

Distributed models of EEG source localization have become increasingly sophisticated. A theoretical advantage of distributed modeling is that its algorithms address the inverse problem with few lead-in assumptions [15]. Standardized low-resolution brain electromagnetic tomography (sLORETA) is one such distributed modeling method. sLORETA can yield 3-dimensional images of electrical neuronal activity with maximum similarities of orientation and strength between neighboring neuronal populations [16]. It is an excellent tool for investigating the electrophysiological and neuroanatomical features of CAE [16–18]; however, only a few studies have investigated the electrophysiological characteristics of CAE by using sLORETA [19]. Thus, to better understand electrophysiological alterations and their development in CAE, we investigated the source origin of epileptiform discharges with a distributed model and performed distributed source localization with sLORETA software.

Materials and methods

Patients and EEG recordings

Sixteen patients (mean age at diagnosis 7.3 years; 6 males, 10 females) with newly diagnosed CAE were recruited before beginning AED treatment in our department. CAE was diagnosed according to the ILAE classification [1], based on clinical history, neurodevelopmental examination, and characteristic EEG findings. No diagnostic procedures or treatments were indicated, missed, or postponed for study purposes. EEG recordings were carried out for 30 min with a Comet® EEG machine (Grass-Telefactor; West Warwick, R.I., USA) at a digitation rate of 200 Hz. Functional trials were performed with rhythmic photo-stimulation (at 3-6-9-12-15-18-21 Hz) and hyperventilation (3 min). Twenty-one silver-silver chloride electrodes were placed according to the international 10-20 system, including the standard 16 temporal and parasagittal scalp sites along with Fz, Cz, Pz, A1, and A2. Additional artifact identification channels were used, including two sites near the eyes, plus respiration and electrocardiography recordings. Eighteen-channel EEG was recorded with a linked ears reference. Additional bipolar derivations were used to differentiate between EEG and eye movement potentials and to detect electromyographic activity. Impedance did not exceed 5 kΩ. In the EEG derivations, the filters were set at 1.0 and 70 Hz. Sixteen-bit online digitization was used.

Table 1 Location of maximal current source density at the midpoint of the ascending phase of 121 epileptiform discharges in 16 patients with childhood absence epilepsy

Lobe		Left	Right	
Frontal (86)	Superior frontal gyrus	13	37	50
	Middle frontal gyrus	5	1	19
	Inferior frontal gyrus	3	4	7
	Medial frontal gyrus	2	45	7
	Precentral gyrus	2		2
	Rectal gyrus		1	1
Temporal (11)	Superior temporal gyrus	2	1	3
	Middle temporal gyrus	1	4	5
	Inferior temporal gyrus	2	1	3
	Angular gyrus			
Parietal (13)	Postcentral gyrus		2	2
	Superior lobule	2	2	4
	Inferior lobule	1	1	2
	Precuneous		4	4
	Inferior parietal gyrus	1		1
Occipital (14)	Middle occipital gyrus	4	1	5
	Inferior occipital gyrus	1		1
	Lingual gyrus	1		1
	Cuneous	1	3	4
		41	80	121

EEG spikes and distributed source localization

Epileptiform discharges were identified by visually inspecting each EEG recording. A total of 121 epileptiform discharges were noted in 16 patients. The number of epileptiform discharges ranged from 1 to 20 per EEG recording (mean ± standard deviation, 7.6 ± 5.2). In each epileptiform discharge, the first discernible prominent spike of the spike-wave complex was selected. From each selected spike, two different EEG epochs were obtained with a time window of 10 ms, including the midpoint of the ascending phase and the negative peak. Thus, a total of 242 EEG epochs were used for distributed source localization with sLORETA software. sLORETA images corresponding to the midpoint of the ascending phase or the negative peak of the spike (121 images each) were obtained from each EEG epoch. The maximum current source density (CSD) location was considered the source origin.

Fig. 1 sLORETA maps of the midpoint of the ascending phase of the spike in Example 1 projected onto brain MRI template slices. Colored areas represent the maximal point (**a**) and spatial extent (**b**) of voxels within the current source density in the brain MRI template slices. The color scale represents sLORETA values. L, left; R, right; A, anterior; P, posterior

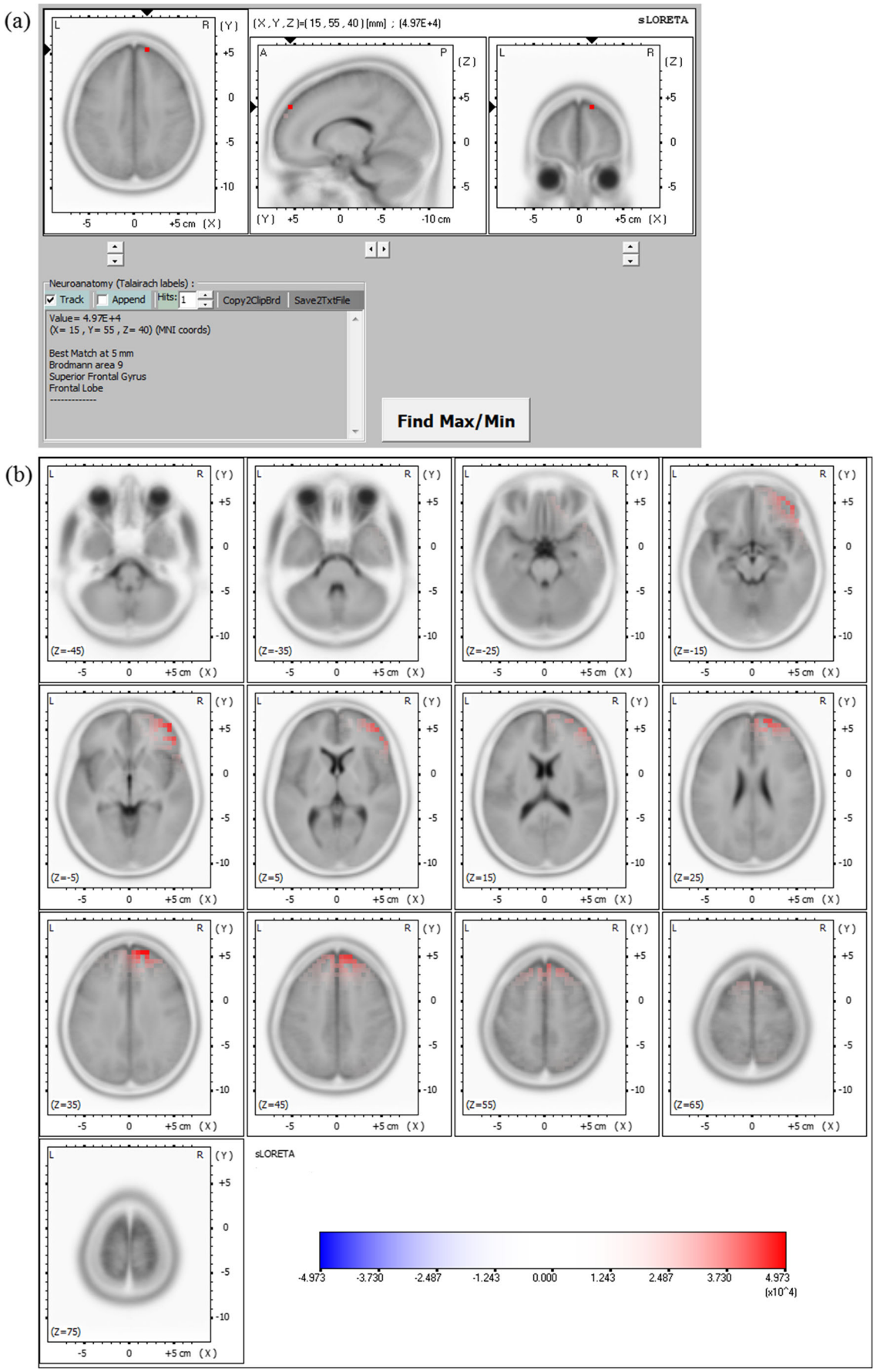
(a)
(X,Y,Z)=(15 , 55 , 40) [mm] ; (4.97E+4)
sLORETA
Neuroanatomy (Talairach labels) :
Track
Append
Hits: 1
Copy2ClipBrd
Save2TxtFile
Value= 4.97E+4
(X= 15 , Y= 55 , Z= 40) (MNI coords)
Best Match at 5 mm
Brodmann area 9
Superior Frontal Gyrus
Frontal Lobe
Find Max/Min
(b)
(Z=-45)
(Z=-35)
(Z=-25)
(Z=-15)
(Z=-5)
(Z=5)
(Z=15)
(Z=25)
(Z=35)
(Z=45)
(Z=55)
(Z=65)
(Z=75)
sLORETA
-4.973
-3.730
-2.487
-1.243
0.000
1.243
2.487
3.730
4.973
(x10^4)

In sLORETA, which is a functional imaging method based on electrophysiological and neuroanatomical constraints, the cortex is modeled as a collection of volume elements (6239 voxels, size 5 × 5 × 5 mm). sLORETA is restricted to the cortical gray matter, hippocampus, and amygdala and uses digitized Montreal Neurological Institute (MNI) coordinates corrected to Talairach coordinates. Neuronal activity is computed as current density ($\mu A/mm^2$) without assuming a predefined number of active sources [16, 20]. Scalp electrode coordinates on the MNI brain were derived from the international 5% system [21]. The sLORETA algorithm solves the inverse problem by assuming related orientations and strengths of neighboring neuronal sources (represented by adjacent voxels). sLORETA has been shown to be an efficient tool for functional mapping because it is consistent with physiology and is capable of correct localization [16]. Additionally, sLORETA localization properties have been independently validated [17, 18].

Results

Source localization at the midpoint of the discharges ascending phase

The maximal CSD was mostly located in the frontal lobe (86 discharges, 71.1%) followed by the parietal lobe (13 discharges, 10.7%). The temporal and occipital lobes were the location of maximal CSD in 11 discharges each (9.1%). At the gyral level, the maximal CSD occurred most frequently in the superior frontal gyrus (50 discharges, 41.3%) followed by the middle frontal gyrus (19 discharges, 15.7%). At the hemisphere level, the maximal CSD was more commonly located in the right hemisphere (80 discharges, 66.1%) than the left (41 discharges, 33.9%).

Table 1 summarizes the maximal CSD at the midpoint of the discharges ascending phase in 16 patients. The exact number and location of the source origins from each patient is reported in the supplemental material. An example of the maximal point and the spatial extent of voxels within the CSD in the brain MRI template slices is shown in Fig. 1. Figure 3a shows examples of spatial extent in the three-dimensional fiducial cortical surface.

Source localization at the negative peak of discharges

The maximal CSD was mostly located in the frontal lobe (82 discharges, 67.8%) followed by the occipital lobe (15 discharges, 12.4%), parietal lobe (14 discharges, 11.6%), and temporal lobe (10 discharges, 8.3%). At the gyral level, the maximal CSD occurred most frequently in the superior frontal gyrus (45 discharges, 37.2%) followed by the middle frontal gyrus (15 discharges, 12.4%) and medial frontal gyrus (14 discharges, 11.6%). At the hemisphere level, the maximal CSD was more commonly located in the right cerebral hemisphere (74 discharges, 61.2%) than the left (47 discharges, 38.8%).

Table 2 Location of maximal current source density at the negative peak of 121 epileptiform discharges in 16 patients with childhood absence epilepsy

Lobe		Left	Right	
Frontal (82)	Superior frontal gyrus	11	34	45
	Middle frontal gyrus	8	7	15
	Inferior frontal gyrus	3	2	5
	Medial frontal gyrus	3	11	14
	Precentral gyrus	1		1
	Rectal gyrus	1	1	2
Temporal (10)	Superior temporal gyrus	1	2	3
	Middle temporal gyrus	3	2	5
	Inferior temporal gyrus	1		1
	angular gyrus		1	1
Parietal (14)	Postcentral gyrus		1	1
	Superior lobule	3		3
	Inferior lobule	2	1	3
	Precuneous	1	5	6
	Inferior parietal Gyrus	1		1
Occipital (15)	Middle occipital gyrus	3	5	8
	Inferior occipital gyrus	1		1
	Lingual gyrus	2		2
	Cuneous	2	2	4
		47	74	121

Table 2 summarizes the maximal points of CSD at the negative peak of discharges in 16 patients. The exact number and location of source origins from each patient is reported in the supplemental material. An example of the maximal point and spatial extent of voxels within the CSD in the brain MRI template slices is shown in Fig. 2. Figure 3b shows examples of spatial extent in the three-dimensional fiducial cortical surface.

Discussion

In this study, we demonstrated that the frontal lobe was the most common origin of epileptiform discharges in CAE. Our results also showed that the frontal lobe was predominant both at the midpoint of the ascending phase and the negative peak of epileptiform discharges. Because the ascending phase of an epileptiform discharge has been considered to be the best

Fig. 2 sLORETA maps of the negative peak of the spike in Example 2 ▶ projected onto brain MRI template slices. Colored areas represent the maximal point (**a**) and spatial extent (**b**) of voxels within the current source density in the brain MRI template slices. The color scale represents sLORETA values. L, left; R, right; A, anterior; P, posterior

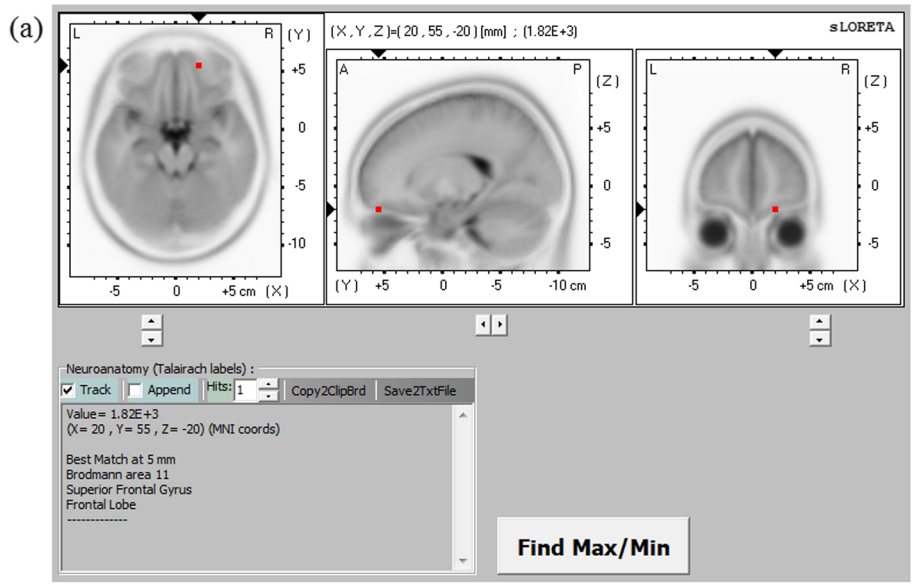
(a)
(X,Y,Z)=(20 , 55 , -20) [mm] ; (1.82E+3)
sLORETA
Neuroanatomy (Talairach labels) :
Track
Append
Hits: 1
Copy2ClipBrd
Save2TxtFile
Value= 1.82E+3
(X= 20 , Y= 55 , Z= -20) (MNI coords)
Best Match at 5 mm
Brodmann area 11
Superior Frontal Gyrus
Frontal Lobe
Find Max/Min

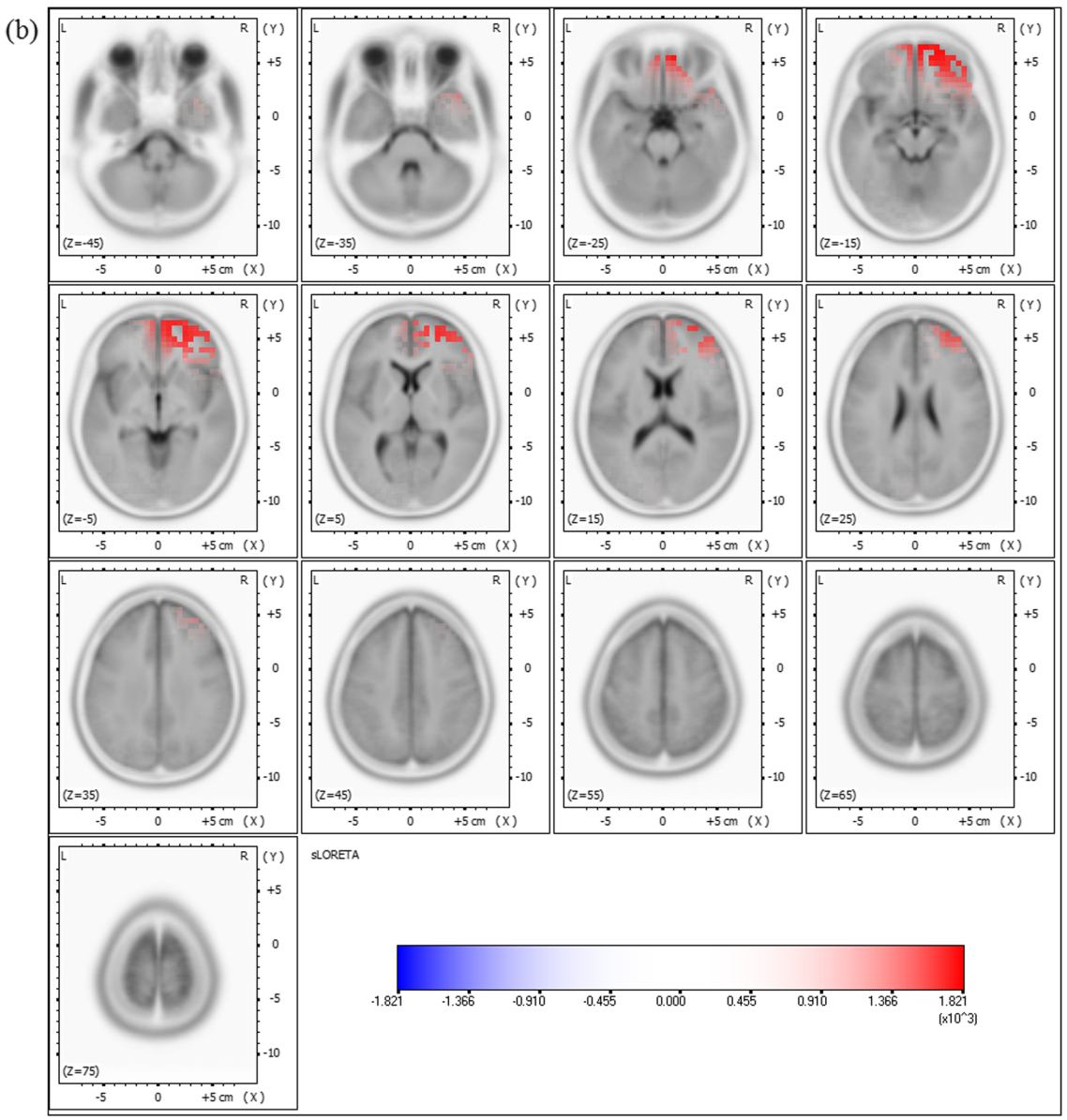
(b)
(Z=-45)
(Z=-35)
(Z=-25)
(Z=-15)
(Z=-5)
(Z=5)
(Z=15)
(Z=25)
(Z=35)
(Z=45)
(Z=55)
(Z=65)
(Z=75)
sLORETA
-1.821
-1.366
-0.910
-0.455
0.000
0.455
0.910
1.366
1.821
(x10^3)

(a)

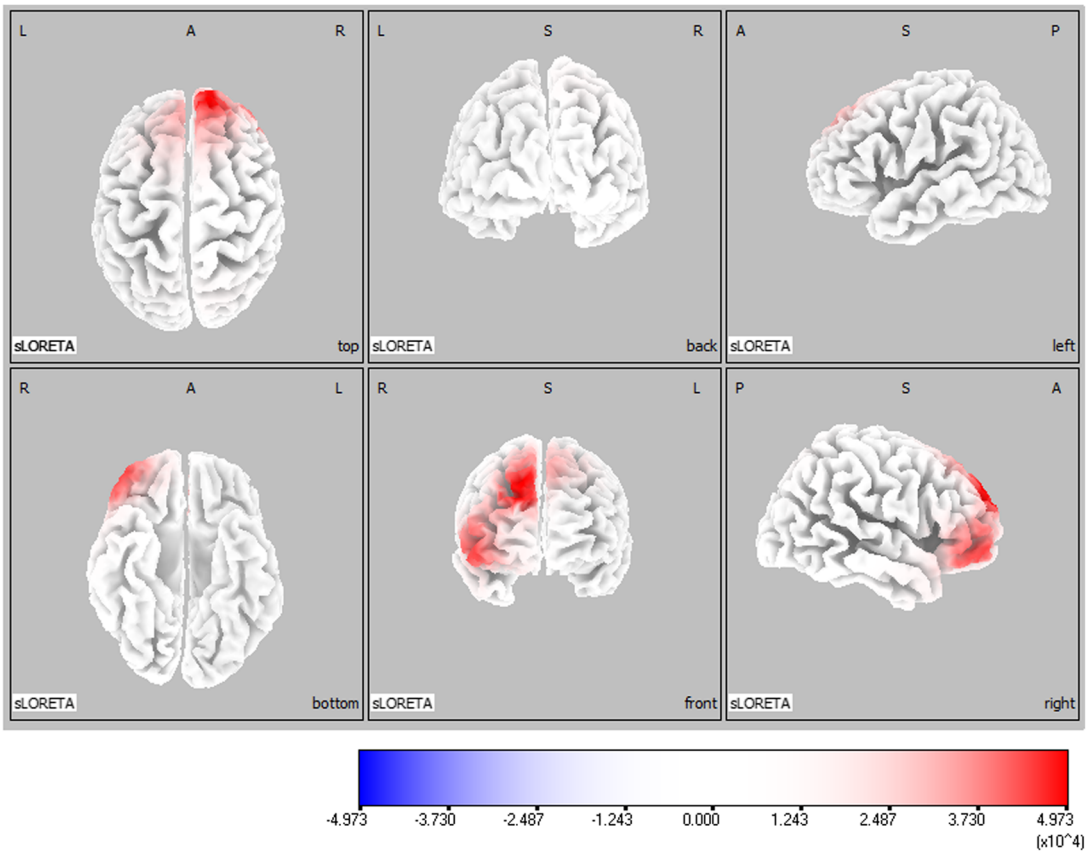
L A R
sLORETA top
L S R
sLORETA back
A S P
sLORETA left
R A L
sLORETA bottom
R S L
sLORETA front
P S A
sLORETA right
-4.973 -3.730 -2.487 -1.243 0.000 1.243 2.487 3.730 4.973
(x10^4)

(b)

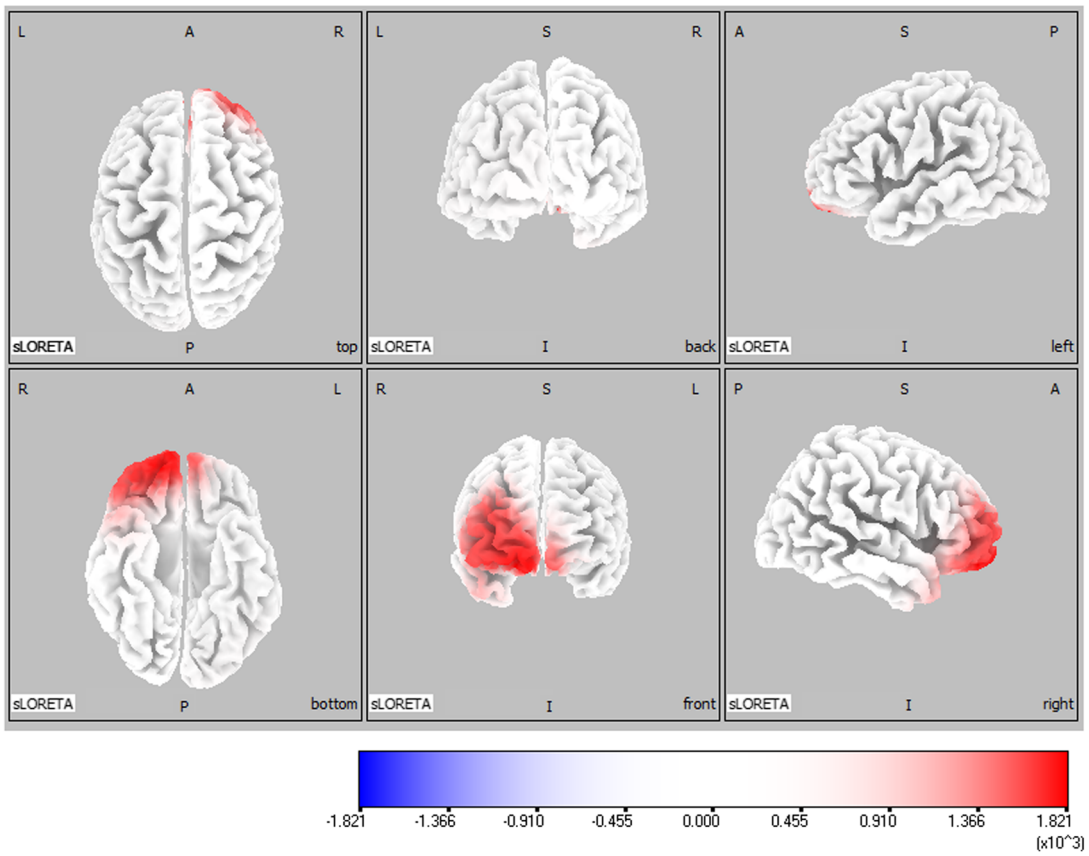
L A R
sLORETA P top
L S R
sLORETA I back
A S P
sLORETA I left
R A L
sLORETA P bottom
R S L
sLORETA I front
P S A
sLORETA I right
-1.821 -1.366 -0.910 -0.455 0.000 0.455 0.910 1.366 1.821
(x10^3)

◀ **Fig. 3** sLORETA maps of the midpoint of the ascending phase of the spike in Example 1 (**a**) and the negative peak of the spike in Example 2 (**b**) projected onto the three-dimensional fiducial brain cortex. Colored areas represent the spatial extent of voxels within the current source density in the three-dimensional fiducial brain cortex. The color scale represents sLORETA values. L, left; R, right; A, anterior; P, posterior; S, superior; I, inferior

timepoint to calculate the spike generator rather than its propagation, we evaluated the source localizations at the negative peak as well as at the ascending phase of epileptiform discharges [22]. Source localization of epileptiform discharges in generalized epilepsy has been a matter of debate and controversy for many years, with recent neuroimaging studies showing that epileptiform discharges in generalized epilepsy are localized to particular regions [23, 24]. Moreover, morphological and metabolic abnormalities of the cerebral cortex do show characteristic topographic patterns in IGE, as revealed by sophisticated neuroimaging [25]. Additionally, some EEG and functional MRI co-registration studies have contributed to understanding the initiation, maintenance, and termination of epileptiform discharges in IGE [26–29].

EEG-based source localization performed as described by Holmes et al. showed evidence of localized medial frontal and frontopolar discharges in absence seizures of five patients with IGE [8]. Furthermore, Anderson et al. and Wandschneider et al. used multimodal neuroimaging analysis methods including EEG, MEG, functional MRI, and diffusion tensor imaging to demonstrate frontal lobe and thalamus activation in IGE [30, 31]. The thalamocortical network is hypothesized to play a crucial role in the fundamental pathogenesis of IGE. Converging evidence suggests a critical role for an abnormal thalamocortical circuit in generating generalized spike and wave complexes. Recent computational advances in neuroimaging have contributed to our understanding of the functional changes in the frontal cortex and thalamus in IGE [32]. In addition, studies investigating IGE have reported structural abnormalities in the frontal lobe on MRI [33–36]. Our findings are consistent with recent studies that have suggested selective cortical involvement, especially in frontal regions, in generalized epilepsy. Moreover, we investigated the initial stages of spike and wave complex bursts, and our results imply that the frontal lobes might be involved in generating spike and wave complexes.

At the gyral level, epileptiform discharges most frequently had a source in the superior frontal gyrus followed by the middle frontal gyrus and medial frontal gyrus. The ascending phase and the negative peak of epileptiform discharges had small differences, but the superior fontal gyrus was the most common origin at both timepoints. Homes et al. proposed that the medial orbitofrontal cortex was specifically involved in IGE [8]. In early neurophysiologic studies, the thalamocortical circuitry was suggested to be regulated by frontothalamic responses, specifically the orbitofrontal cortex [37, 38]. However, other regions of the frontal lobe may also be involved in the spike and wave complex of IGE [30, 31]. Gadad et al. reported that epileptiform discharges in IGE were most commonly localized in the middle frontal gyrus at the peak [12]. Moreover, the source location might vary according to IGE subtype based on the duration of the spike and wave complexes [12]. We demonstrated that the source location was predominantly in the right hemisphere in CAE and that the right cerebral hemisphere was dominant in 63.6% of patients. Stefan et al. reported right side localization in 10 of 13 seizure episodes in a cohort of seven patients with IGE [39]. However, variable patterns of IGE subtypes were observed. Moreover, this cohort did not include patients with CAE. In essence, the exact source location in IGE varies among studies, and little is known about the origin, particularly in CAE.

Additionally, our results showed some variations in source localization in CAE within a patient as well as between patients (refer to the supplementary material). Moeller et al. reported patient-specific, but not region-specific, signal changes in functional MRI studies of absence seizures [28]. However, our study showed that particular regions predominate in CAE, especially the frontal lobe, although there were variations within and between patients.

To our knowledge, this is the first study to investigate the source of epileptiform discharges by using a distributed model in CAE only. We found that the source was located predominantly in the frontal lobe, suggesting that the frontal lobe might be involved in generating CAE. This result is consistent with previous studies that have proposed selective cortical involvement, especially of frontal regions, in IGE. Furthermore, we described the distinctive features of source localization in CAE.

A limitation of this study is the small number of patients. A larger sample size is needed to make the results more generalizable. Additionally, analysis with sLORETA is restricted to the cortical gray matter, hippocampus, and amygdala [20]. Therefore, deep subcortical structures such as the thalamus were not considered in the analysis. sLORETA is an excellent tool with no location bias, but other neuroimaging analysis techniques could also be considered. Thus, extended studies with a larger sample size and other analysis tools are needed to confirm our findings.

In conclusion, we demonstrated selective cortical involvement of frontal regions in epileptiform discharges as well as distinctive source patterns in CAE. These findings enhance our understanding of electrophysiological changes and their development in CAE.

Compliance with ethical standards

Conflict of interest The authors declare that they have no conflicts of interest.

Publisher's note Springer Nature remains neutral with regard to jurisdictional claims in published maps and institutional affiliations.

References

1. Scheffer IE, Berkovic S, Capovilla G et al (2017) ILAE classification of the epilepsies: position paper of the ILAE Commission for Classification and Terminology. Epilepsia 58:512–521
2. Panayiotopoulos CP (2010) Idiopathic generalised epilepsies. In: Panayiotopoulos CP (ed) A clinical guide to epileptic syndromes and their treatment, revised, 2nd edn. Springer, London, pp 377–422
3. Morison RS, Dempsey EW (1941) A study of thalamo-cortical relations. Am J Phys 135:281–292
4. Jasper HH, Droogleever-Fortuyn J (1946) Experimental studies on the functional anatomy of petit mal epilepsy. Res Publ Assoc Res Nerv Ment Dis 26:272–298
5. McCormick DA (2002) Cortical and subcortical generators of normal and abnormal rhythmicity. Int Rev Neurobiol 49:99–114
6. Slaght SJ, Leresche N, Deniau JM, Crunelli V, Charpier S (2002) Activity of thalamic reticular neurons during spontaneous genetically determined spike and wave discharges. J Neurosci 22: 2323–2334
7. Shahar E, Andraus J, Sagie-Lerman T, Savitzki D (2002) Valproic acid therapy inducing absence status evolving into generalized seizures. Pediatr Neurol 26:402–404
8. Holmes MD, Brown M, Tucker DM (2004) Are "generalized" seizures truly generalized? Evidence of localized mesial frontal and frontopolar discharges in absence. Epilepsia 45:1568–1579
9. Niedermeyer E (2005) Epileptic seizure disorders. In: Niedermeyer E, Lopes da Silva F (eds) Electroencephalography: basic principles, clinical applications, and related fields, 5th edn. Lippincott Williams & Wilkins, Philadelphia, pp 505–620
10. Goldensohn ES, Legatt AD, Koszer S, Wolf SM (1999) Goldensohn's EEG interpretation: problems of overreading and underreading, 2nd edn. Futura Publishing, New York
11. Panayiotopoulos CP (1994) The clinical spectrum of typical absence seizures and absence epilepsies. In: Malafosse A, Genton P, Hirsch E et al (eds) Idiopathic generalized epilepsies: clinical, experimental, genetic aspects. John Libbey, London, pp 75–85
12. Gadad V, Sinha S, Mariyappa N, Velmurugan J, Chaitanya G, Saini J, Thennarasu K, Satishchandra P (2018) Source analysis of epileptiform discharges in absence epilepsy using magnetoencephalography (MEG). Epilepsy Res 140:46–52
13. Cortez MA, Kostopoulos GK, Snead OC 3rd (2016) Acute and chronic pharmacological models of generalized absence seizures. J Neurosci Methods 260:175–184
14. Yeni SN, Kabasakal L, Yalçinkaya C, Nisli C, Dervent A (2000) Ictal and interictal SPECT findings in childhood absence epilepsy. Seizure 9:265–269
15. Plummer C, Wagner M, Fuchs M, Vogrin S, Litewka L, Farish S, Bailey C, Harvey AS, Cook MJ (2010) Clinical utility of distributed source modelling of interictal scalp EEG in focal epilepsy. Clin Neurophysiol 121:1726–1739
16. Pascual-Marqui RD (2002) Standardized low-resolution brain electromagnetic tomography (sLORETA): technical details. Methods Find Exp Clin Pharmacol 24(Suppl D):5–12
17. Wagner M, Fuchs M, Kastner J (2004) Evaluation of sLORETA in the presence of noise and multiple sources. Brain Topogr 16:277–280
18. Sekihara K, Sahani M, Nagarajan SS (2005) Localization bias and spatial resolution of adaptive and non-adaptive spatial filters for MEG source reconstruction. Neuroimage 25:1056–1067
19. Shin JH, Eom TH, Kim YH, Chung SY, Lee IG, Kim JM (2017) Comparative analysis of background EEG activity in childhood absence epilepsy during valproate treatment: a standardized, low-resolution, brain electromagnetic tomography (sLORETA) study. Neurol Sci 38:1293–1298
20. Fuchs M, Kastner J, Wagner M, Hawes S, Ebersole JS (2002) A standardized boundary element method volume conductor model. Clin Neurophysiol 113:702–712
21. Jurcak V, Tsuzuki D, Dan I (2007) 10/20, 10/10, and 10/5 systems revisited: their validity as relative head-surface-based positioning systems. Neuroimage 34:1600–1611
22. Lantz G, Spinelli L, Seeck M, de Peralta Menendez RG, Sottas CC, Michel CM (2003) Propagation of interictal epileptiform activity can lead to erroneous source localizations: a 128-channel EEG mapping study. J Clin Neurophysiol 20:311–319
23. Gadad V, Sinha S, Mariyappa N, Chaithanya G, Jayabal V, Saini J, Thennarasu K, Satishchandra P (2017) Source localization of epileptiform discharges in juvenile myoclonic epilepsy (JME) using magnetoencephalography (MEG). Epilepsy Res 129:67–73
24. Clemens B, Bessenyei M, Piros P, Tóth M, Seress L, Kondákor I (2007) Characteristic distribution of interictal brain electrical activity in idiopathic generalized epilepsy. Epilepsia 48:941–949
25. Koepp MJ, Duncan JS (2004) Epilepsy. Curr Opin Neurol 17:467–474
26. Bai X, Vestal M, Berman R, Negishi M, Spann M, Vega C, Desalvo M, Novotny EJ, Constable RT, Blumenfeld H (2010) Dynamic time course of typical childhood absence seizures: EEG, behavior, and functional magnetic resonance imaging. J Neurosci 30:5884–5893
27. Carney PW, Masterton RA, Harvey AS et al (2010) The core network in absence epilepsy. Differences in cortical and thalamic BOLD response. Neurology 75:904–911
28. Moeller F, LeVan P, Muhle H, Stephani U, Dubeau F, Siniatchkin M, Gotman J (2010) Absence seizures: individual patterns revealed by EEG-fMRI. Epilepsia 51:2000–2010
29. Benuzzi F, Mirandola L, Pugnaghi M, Farinelli V, Tassinari CA, Capovilla G, Cantalupo G, Beccaria F, Nichelli P, Meletti S (2012) Increased cortical BOLD signal anticipates generalized spike and wave discharges in adolescents and adults with idiopathic generalized epilepsies. Epilepsia 53:622–630
30. Anderson J, Hamandi K (2011) Understanding juvenile myoclonic epilepsy: contributions from neuroimaging. Epilepsy Res 94:127–137
31. Wandschneider B, Thompson PJ, Vollmar C, Koepp MJ (2012) Frontal lobe function and structure in juvenile myoclonic epilepsy: a comprehensive review of neuropsychological and imaging data. Epilepsia 53:2091–2098
32. Kim JB, Suh SI, Seo WK, Oh K, Koh SB, Kim JH (2014) Altered thalamocortical functional connectivity in idiopathic generalized epilepsy. Epilepsia 55:592–600
33. Betting LE, Mory SB, Lopes-Cendes I, Li LM, Guerreiro MM, Guerreiro CAM, Cendes F (2006) MRI reveals structural abnormalities in patients with idiopathic generalized epilepsy. Neurology 67: 848–852
34. Pardoe H, Pell GS, Abbott DF, Berg AT, Jackson GD (2008) Multi-site voxel-based morphometry: methods and a feasibility demonstration with childhood absence epilepsy. Neuroimage 42:611–616
35. Caplan R, Levitt J, Siddarth P, Wu KN, Gurbani S, Sankar R, Shields WD (2009) Frontal and temporal volumes in childhood absence epilepsy. Epilepsia 50:2466–2472
36. Tondelli M, Vaudano AE, Ruggieri A, Meletti S (2016) Cortical and subcortical brain alterations in juvenile absence epilepsy. Neuroimage Clin 12:306–311
37. Morrison R, Dempesy E (1942) A study of thalamocortical relations. Am J Phys 135:281–292
38. Morrison R, Dempesy E (1943) Mechanism of thalamocortical augmentation and repetition. Am J Phys 138:297–308
39. Stefan H, Paulini-Ruf A, Hopfengärtner R, Rampp S (2009) Network characteristics of idiopathic generalized epilepsies in combined MEG/EEG. Epilepsy Res 85:187–198